

TOPICAL REVIEW

Comparisons of microwave dielectric property measurements by transmission/reflection techniques and resonance techniques

Jyh Sheen

Department of Electronic Engineering, National Formosa University, Hu-Wei, Yun-Lin 632, Taiwan, Republic of China

E-mail: jsheen@nfu.edu.tw

Received 15 October 2007, in final form 22 February 2008

Published 27 January 2009

Online at stacks.iop.org/MST/20/042001

Abstract

This review provides a general comparison of the two most commonly used techniques for measurement of complex permittivity at microwave frequencies: transmission/reflection and resonance. The transmission/reflectance techniques are analyzed using distributed and lumped impedance models. The resonance techniques are analyzed using both dielectric and cavity resonance models. The analysis, combined with experimental results, enables us to illustrate the advantages and disadvantages of the various techniques and provide guidance on which techniques to use under particular circumstances. In general, transmission/reflection techniques can be used over a broad band of frequencies, and are suitable for loss measurements on high loss materials. Resonance techniques do not have swept frequency capability, but have higher accuracy for measurement of the real part of permittivity and can measure the loss tangent of low loss materials with high resolution.

Keywords: microwave measurements, resonance technique, transmission technique, reflection technique, dielectric constant, dielectric loss, loss tangent, complex permittivity

1. Introduction

Various techniques are widely used for measurements of microwave dielectric properties (relative complex permittivity, $\varepsilon = \varepsilon_r - j\varepsilon_c$), i.e. real part (ε_r) and loss tangent ($\tan \delta = \varepsilon_c/\varepsilon_r$). The correct choice of microwave measurement techniques is important as various microwave measurement techniques are available and various restrictions exist in the techniques. The choice of adequate measurement techniques would depend on the values of real and imaginary parts of permittivity and the shape and dimension of the measured sample. An ideal method includes the following merits.

(1) It has good measurement accuracy for both/either ε_r and/or $\tan \delta$.

- (2) The measurement procedures are simple and easy.
- (3) The required sample dimension is small (or nondestructive measurement).
- (4) The measured frequency range is as wide as possible and it has the swept frequency capability.

Some good overviews of the microwave measurement techniques of dielectric properties have been given previously [1–4]. A review of a specific area was also studied [5]. However, there are too many techniques to be covered in a single article. In addition to the general review, a further comparison of two widely used types of measurement techniques at microwave frequencies is the goal of this paper.

The two types of microwave measurement techniques are (i) transmission/reflection techniques and (ii) resonance

techniques. Transmission/reflection techniques can be used to obtain the real part of permittivity of a high or low loss specimen, but lack the resolution to measure low loss tangents. Resonant techniques are only suitable for low loss material since the resonance curve broadens as the loss increases. Usually, dielectric property measurements by the resonance techniques have higher accuracy than measurements by the transmission/reflection techniques especially for the loss measurement. In addition, the transmission/reflection techniques usually have the swept frequency ability for the measured frequency range. The transmission and/or reflection signals are always tested to calculate the dielectric properties of the specimen. Unlike the transmission/reflection techniques, the resonance techniques do not have the swept frequency capability. Only one or certain frequency points can be measured. These techniques typically require two port measurements of S -parameters with instruments such as vector network analyzers.

The transmission/reflection techniques can be further divided into two categories. The first is the distributed impedance method, in which the S_{11} and/or S_{21} parameters are measured for the calculations of dielectric properties. The other is the lumped impedance method, in which the calculations of dielectric properties are based on circuit theory and the electric field in the measured sample is assumed to be uniform, i.e. under a low frequency condition.

Like the transmission/reflection techniques, the resonance techniques can be further divided into two categories. The first is that the resonance is basically supported by the dielectric sample itself. The sample acts as a dielectric resonator. Metal shields with different geometries are always introduced to prevent radiation loss. This type is called the dielectric resonance technique. The second type is that the resonance is supported by the metal walls of a metal cavity. The presence of a sample in the cavity causes only a ‘perturbation’ in the field distributions in the metal cavity. The second type is called the cavity resonance technique. For the dielectric resonance technique, the lowest TE mode of a cylindrical dielectric sample is always used for measurements because it is easier to identify the resonant peak, and the calculation equations for the dielectric properties are more easily derived than those of other modes. The main advantage of the dielectric resonance methods is the higher accuracy of measurements, but there are several disadvantages. Usually, only a single frequency point can be measured for each sample. The dielectric resonance techniques do not have the swept frequency capability. In addition, the calculations of dielectric properties are always quite complicated; a computer program is required to deal with the complicated Bessel functions. A further disadvantage is the requirement of sample dimension; a much larger sample volume is needed than that for the cavity resonance techniques. However, the dielectric resonance techniques are still widely used because of higher accuracy of dielectric property measurements, especially for loss measurements.

In this paper, a general review and comparison of the above measurement techniques will be given. Experiments will be conducted on some chosen measurement methods

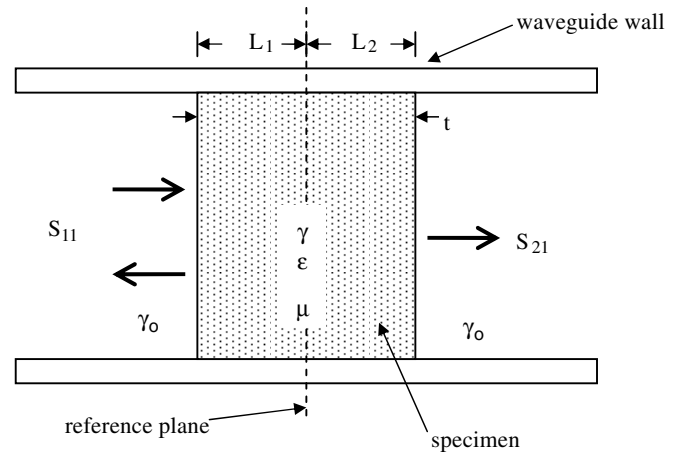


Figure 1. Distributed transmission technique.

to compare and understand the limitations of microwave dielectric properties by various measurement methods.

2. Study of measurement techniques

2.1. Transmission/reflection techniques

There are various transmission/reflection techniques for measuring the dielectric properties of dielectric samples [6–20]. As mentioned, the main advantage of the transmission/reflection techniques is the swept frequency capability and transmission/reflection techniques can be further divided into two categories—the distributed impedance method and the lumped impedance method.

2.1.1. Distributed impedance techniques. A dielectric slab or disk can be bounded by a sample holder for the distributed transmission method, as shown in figure 1, where a rectangular microwave waveguide is adopted as the holder. (Coaxial lines can be used instead of a waveguide as the sample holder. They bring the advantage of a wider frequency band, although errors due to air gaps are generally larger.) The arrows in this figure and the following figures indicate the directions of signal flow and the measurement parameters—transmission signal (S_{21}) and reflection signal (S_{11}). The S_{11} and S_{21} parameters can be expressed as [6–9]

$$S_{11} = R_1^2 \Gamma \frac{1 - z^2}{1 - \Gamma^2 z^2} \quad (1)$$

$$S_{22} = R_2^2 \Gamma \frac{1 - z^2}{1 - \Gamma^2 z^2} \quad (2)$$

$$S_{21} = R_1 R_2 z \frac{1 - \Gamma^2}{1 - \Gamma^2 z^2} \quad (3)$$

$$R_1 = e^{\gamma_0 L_1}, \quad R_2 = e^{\gamma_0 L_2}, \quad z = e^{-\gamma t} \quad (4)$$

$$\Gamma = \frac{\gamma_0/\gamma - 1}{\gamma_0/\gamma + 1} \quad (5)$$

$$\gamma = \sqrt{k_c^2 - \epsilon k_0^2}, \quad \gamma_0 = \sqrt{k_c^2 - k_0^2}, \quad k_0 = \omega \sqrt{\mu \epsilon_0}, \quad (6)$$

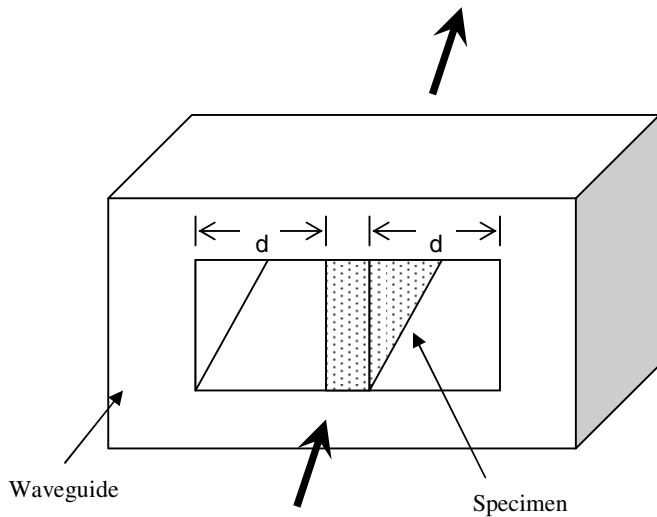


Figure 2. Longitudinal transmission technique.

where t is the sample thickness, γ is the propagation constant in the sample, Γ is the reflection coefficient on the air/dielectric boundary and k_c is the waveguide cutoff wavenumber. The above equations can be used for the calculations of ϵ_r and $\tan \delta$.

Equations (1) to (6) may be solved for complex permittivity using the Nicolson–Ross–Weir method [10, 11] from measurements of both S_{11} and S_{21} . However, this approach is numerically unstable at frequencies at which the specimen is a multiple of one half-wavelength in length [6, 7, 12]. A more satisfactory approach is to use an iterative technique. This enables a value of permittivity [6–8] to be determined from each S -parameter S_{11} , S_{21} , etc, for a non-magnetic specimen. S_{21} and S_{12} measurements tend to yield complex permittivity results with a smaller uncertainty than S_{11} or S_{22} . A further reason for preferring S_{21} and S_{12} measurements is that the specimen position in the transmission line need not be known. Uncertainties vary with wavelength and are generally lowest for specimens of thickness $\lambda/4$, $3\lambda/4$, etc, and greatest for thickness $\lambda/2$, λ , etc. The resolution for loss tangent is approximately 10^{-2} . For magnetic specimens, S_{21} and S_{11} must both be measured and both complex permittivity and permeability must be calculated. This can also be done iteratively.

A different configuration for the measurement of complex permittivity is shown in figure 2 [13, 14]. The characteristic equation for an inhomogeneous filled rectangular waveguide with very thin sample thickness is [11]

$$\tan [d(k_o^2 - \gamma^2)] \tan [\frac{1}{2}c(\epsilon k_o^2 - \gamma^2)] = \sqrt{\frac{k_o^2 - \gamma^2}{\epsilon k_o^2 - \gamma^2}}. \quad (7)$$

The calculation formulae of this longitudinal transmission configuration for the real part (ϵ_r) and imaginary part (ϵ_e) of complex permittivity ($\epsilon = \epsilon_r - j\epsilon_e$) can then be derived from the above equation [13]. However, this technique is only adequate for dielectric property measurements of low ϵ_r materials [13].

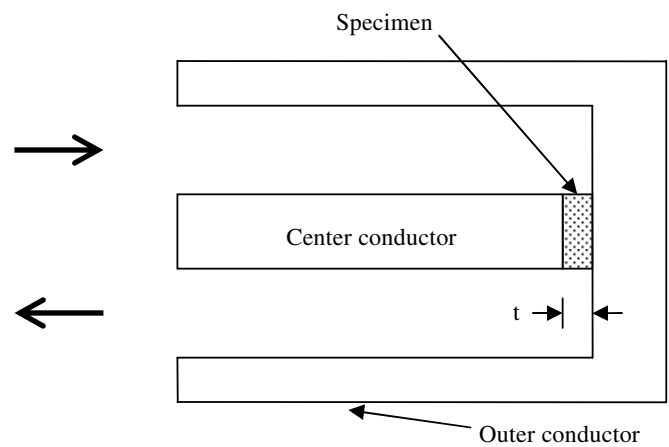


Figure 3. Lumped impedance technique.

2.1.2. *Lumped impedance technique.* A small disk-shaped and electroded sample is placed at the end of a shorted coaxial line, as shown in figure 3. Complex reflection coefficients are measured by the impedance analyzer or network analyzer. By neglecting the effect of fringing field, ϵ_r and $\tan \delta$ can be obtained by the formula of complex reflection coefficients [21–24]

$$\Gamma = |\Gamma| e^{-j\theta} = \frac{1 - j\omega C_o Z_o \epsilon}{1 + j\omega C_o Z_o \epsilon}, \quad (8)$$

where $C_o = A\epsilon_o/t$ is the free space capacitance, A is the sample area, t is the sample thickness, Z_o is the characteristic impedance of the coaxial line, ϵ is the complex relative permittivity, ϵ_o is the free space permittivity value and Γ is the complex reflection coefficient with amplitude $|\Gamma|$ and phase θ .

The lumped impedance method assumes that the electric field is uniform throughout the sample. Calculations of dielectric properties are based on the circuit theory. Therefore, measurements of high ϵ_r material or at high frequencies are not adequate. The measurement limitation on loss tangent is about the same as for the distributed method.

2.2. Dielectric resonance techniques

There are various dielectric resonance techniques for measuring the dielectric properties of dielectric samples [25]. The differences among these techniques are based on different geometrical arrangements of metal shields and signals measured. The measured signal can be transmission (S_{21}) or reflection (S_{11}). The transmission measurements are normally made with weak coupling to minimize uncertainties of Q -factor in the following, whereas reflection measurements are always made with strong coupling [26, 27].

One popular dielectric resonance method is the Hakki–Coleman resonance method, where a cylindrical dielectric rod is placed between two parallel metal plates as shown in figure 4. Two coupling antennas are used to couple the power in and out. The measured parameter is S_{21} . The TE_{011} mode is adopted for measurements. The real part of permittivity is calculated by the relationship between the resonant frequency and sample dimensions [28–31].

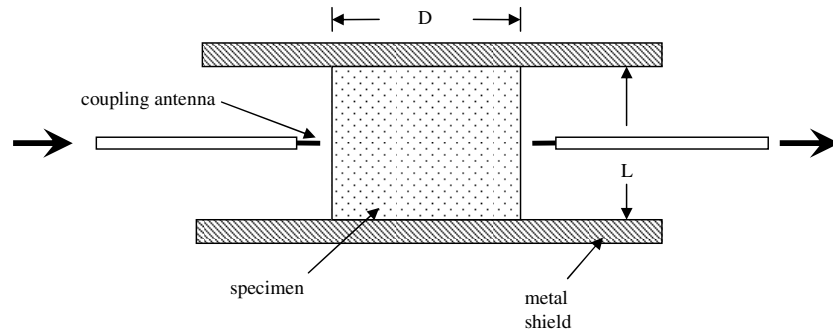


Figure 4. Hakki-Coleman resonance technique.

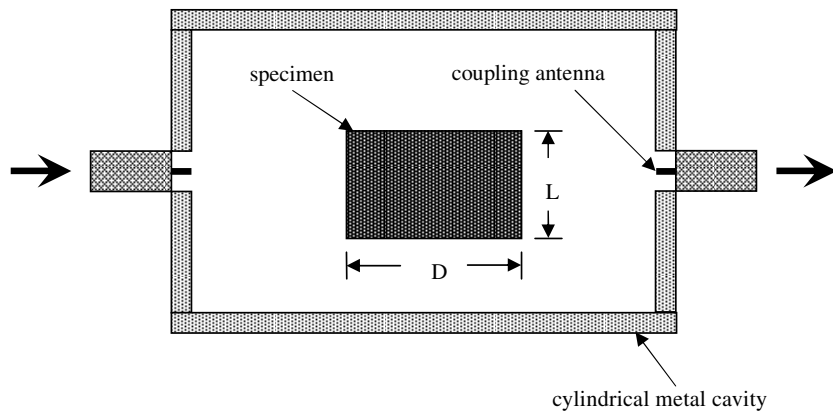


Figure 5. Cylindrical cavity resonance technique.

The computation of loss tangent is given by [25–39]

$$\tan \delta = A \left(\frac{1}{Q_u} - \frac{1}{Q_c} - \frac{1}{Q_r} \right), \quad (9)$$

where Q_u is the measured unloaded quality factor, Q_c is the quality factor due to conductor loss and Q_r is the quality factor due to radiation loss. The factor A is the ratio of total energy stored in the dielectric and air to the energy stored in the dielectric. Usually, the A factor is very close to 1 for ϵ_r larger than 20. The radiation loss can be neglected in measurement. The accurate calculation of Q_c is a critical point for the correct measurement of loss tangent by this method. Loss tangent values less than 5×10^{-4} should not be measured by the Hakki-Coleman resonance method unless the surface resistance value can be precisely determined for calculation of Q_c [28, 29]. Loss tangents can then be measured down to about 1×10^{-4} .

The real part of permittivity is calculated by the dielectric/air boundary condition [28–31]:

$$\frac{J_0(k_{ci}a)}{J_1(k_{ci}a)} = -\frac{k_{co}a}{k_{ci}a} \frac{K_0(k_{co}a)}{K_1(k_{co}a)}, \quad (10)$$

where a is the radius of sample, k_{ci} and k_{co} are the wavenumbers of r direction for $r < a$ and $r > a$, respectively, and they are ϵ_r and sample geometry dependent. J and K are Bessel function and modified Bessel function, respectively.

The other measurement configuration is the cylindrical cavity structure as shown in figure 5 [32, 33, 40–43]. The sample under test is put inside a cylindrical metal cavity. The $TE_{01\delta}$ mode is used for measurement. The loss tangent is

calculated by

$$\tan \delta = A \left(\frac{1}{Q_u} - \frac{1}{Q_c} \right) \quad (11)$$

with the A factor very close to 1. By comparison with equation (9), the sample is located inside a closed cavity; therefore there is no radiation loss. Since the sample is not in contact with the metal shields, the conductor loss is much lower than that of the Hakki-Coleman technique. The accuracy for loss measurement is higher. In addition, the sample dimension requirement is smaller than that for the Hakki-Coleman technique. Figure 6 gives the relationship between the resonant frequency and the sample dimensions of the Hakki-Coleman and the cylindrical cavity structures. For the cylindrical cavity structure in the figure, the air gaps above and below the sample are both equal to 5 mm. For a sample with $\epsilon_r = 20$, measured at 10 GHz, $D \times L$ is about 6 mm \times 3 mm—much smaller than the 10 mm \times 5 mm requirement for the Hakki-Coleman method. One disadvantage of this method is that the specimen is put inside a closed cavity; the desired $TE_{01\delta}$ mode may become mixed with the other modes supported by the metal cavity.

The dielectric/air boundary condition for measurement of the real part of permittivity in figure 5 is [44]

$$\frac{J_0(k_{ci}a)}{J_1(k_{ci}a)} = -\frac{k_{co}a}{k_{ci}a} \frac{1}{K_1(k_{co}a)} \left[K_0(k_{co}a) + \frac{1}{k_{co}a} K_1(k_{co}b) \right], \quad (12)$$

where b is the radius of the metal cavity.

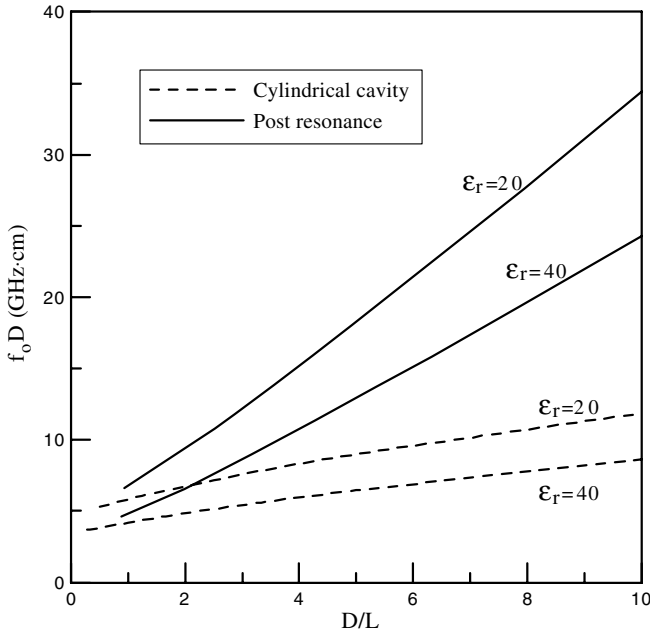


Figure 6. A graph showing the relationship between the resonant frequency and the sample dimensions of the Hakki–Coleman and the cylindrical cavity structures. For the cylindrical cavity structure, the air gaps above and below the sample are both equal to 5 mm.

In contrast to the above two techniques where the transmission signal (S_{21}) is taken, a reflection cavity dielectric resonance technique can be used in which case the reflection signal is measured, i.e. the S_{11} parameter. The configuration is shown in figure 7. The sample is usually put inside a rectangular cavity with one end shorted and adjustable for the best resolution of the resonance signal. The $TE_{01\delta}$ mode is also used for this method. Like the cylindrical cavity method, this technique has been used for low loss measurement [45, 46]. Equation (11) is also used for the calculation of loss tangent. The measured unloaded Q is calculated by using the expression [26]

$$Q_u = \left(\frac{P_x - P_{\min}}{P_{\max} - P_x} \right)^{1/2} \frac{2}{2 \pm \sqrt{P_{\min}} - \sqrt{P_{\max}}} \frac{f_0}{\Delta f_x} \quad (13)$$

The \pm sign accounts for the undercoupled case (+) and overcoupled case (–) and $P_{\max} \approx 1$. The characteristics of this technique are very similar to those of the cylindrical cavity resonance technique except that the measurement error of the reflection method is higher than that of the cylindrical cavity technique because of the uncertainty condition [25]. The required sample dimension is about the same size as that of the cylindrical cavity structure.

The dielectric/air boundary condition for the measurement of the real part of permittivity in figure 7 is [47]

$$\frac{J_0(k_{ci}a)}{J_1(k_{ci}a)} = -\frac{k_{co}a}{k_{ci}a} \frac{1}{K_1(k_{co}a)} \left[K_0(k_{co}a) + \frac{1}{2k_{co}a} K_1(k_{co}b) \right], \quad (14)$$

where $2b$ is the width of the waveguide cross section. The frequency limitations of figures 4, 5 and 7 will depend on

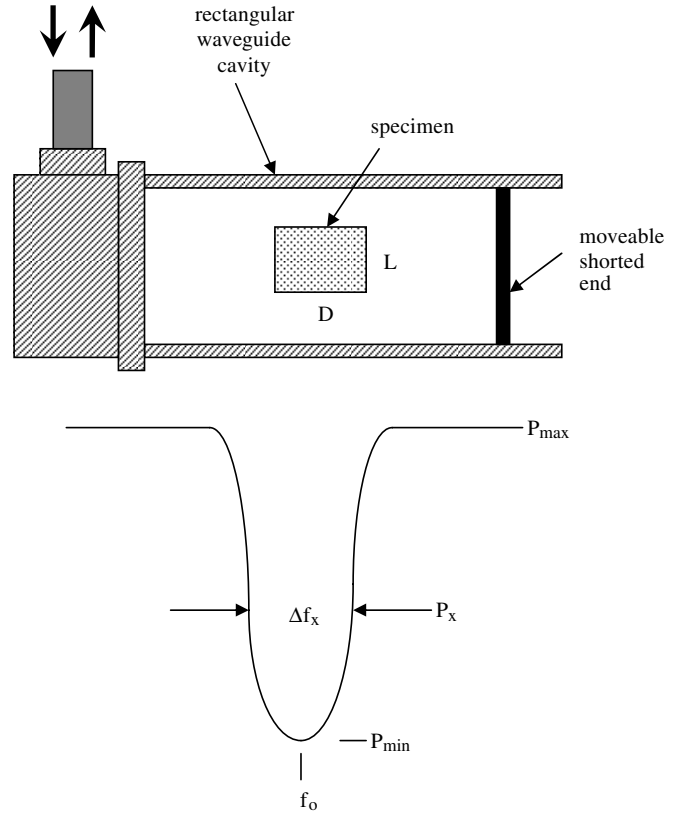


Figure 7. Waveguide reflection resonance technique.

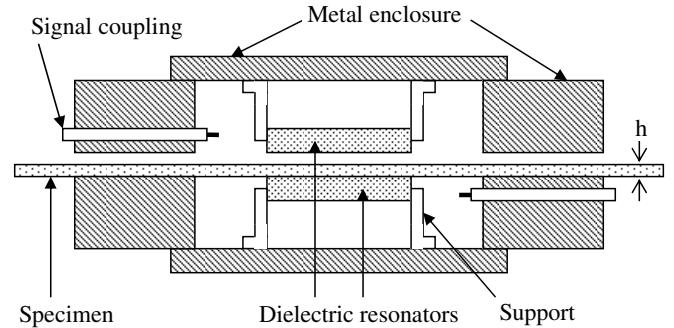


Figure 8. Split-post dielectric resonator technique.

ϵ_r and can be determined by equations (10), (12) and (14), respectively.

In addition to the above traditional $TE_{01\delta}$ type dielectric resonator methods, a very useful dielectric resonance method is the split-post dielectric resonator technique shown in figure 8. The split-post dielectric resonator provides a convenient, accurate and nondestructive measurement of a substrate and printed circuit board. The real part of complex permittivity can be calculated by [40, 48–50]

$$\epsilon_r = 1 + \frac{f_0 - f_s}{hf_0 K_s(\epsilon_r, h)}, \quad (15)$$

where h is the sample thickness, f_0 is the resonant frequency without the sample and f_s is the resonant frequency with the sample. K_s is a function of ϵ_r and h related. It is pre-computed and tabulated for a number of ϵ_r and h . Interpolation is then

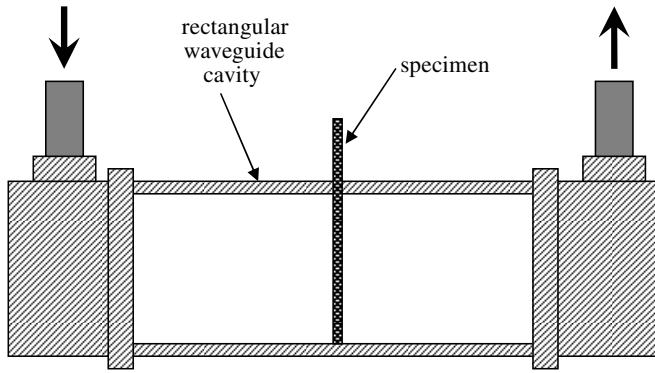


Figure 9. TE cavity perturbation technique.

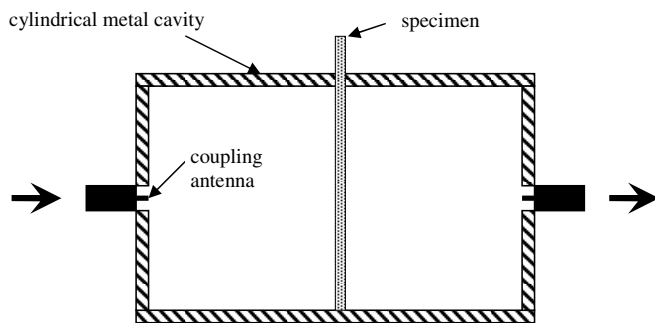


Figure 10. TM cavity perturbation technique.

used to compute K_s for specific permittivity and thickness values.

For the computation of the loss tangent, equation (9) is modified to [40, 48–50]

$$\tan \delta = A \left(\frac{1}{Q_u} - \frac{1}{Q_c} - \frac{1}{Q_r} - \frac{1}{Q_d} \right), \quad (16)$$

where the extra term Q_d is the quality factor due to the loss of dielectric resonators and the energy factor A is the ratio of the total energy stored in the resonant measurement fixture to the energy stored in the sample.

2.3. Cavity resonance technique

A small dielectric sample in the resonant cavity will cause a shift of the resonant frequency and a decrease of the quality factor of the cavity. The complex permittivity of the specimen can then be calculated from the changes of the resonant frequency and quality factor of the metal cavity. The cavity can be either rectangular or cylindrical as shown in figures 9 and 10. The sample is always located where the electric field is maximum for testing.

2.3.1. Rectangular cavity. The TE_{01N} (N integer) modes are widely used for dielectric property measurements. A small piece of rod, sheet or bar-shaped sample is located in the position of the maximum electric field. For odd modes (N : odd), the geometrical center is always one of the maximum electric field positions. ϵ_r and $\tan \delta$ of the specimen can then be calculated from the changes of the resonant frequency and

quality factor of the metal cavity, respectively [51, 52]

$$\epsilon_r = \frac{V_c(f_c - f_s)}{2V_s f_s} + 1 \quad (17)$$

$$\epsilon_c = \frac{V_c}{4V_s} \left(\frac{1}{Q_s} - \frac{1}{Q'_c} \right) \quad (18)$$

$$Q'_c = Q_c \left[1 + (\epsilon_r - 1) \frac{V_s}{V_c} \right], \quad (19)$$

where f_c and f_s are the resonant frequencies, Q_c and Q_s are the quality factors of the cavity without and with the sample inside the cavity, respectively, and V_c and V_s are the volumes of the cavity and sample, respectively.

2.3.2. Cylindrical cavities. For cylindrical cavities, the TM_{010} mode is usually used. The sample is located along its symmetric axis in the position of the maximum electric field strength for ease of measurement and calculation as shown in figure 10. ϵ_r and $\tan \delta$ of the specimen can then be calculated by [15, 51, 53, 54]

$$\epsilon_r = 0.539 \frac{V_c(f_c - f_s)}{V_s f_s} + 1 \quad (20)$$

$$\epsilon_c = 0.269 \frac{V_c}{V_s} \left(\frac{1}{Q_s} - \frac{1}{Q'_c} \right). \quad (21)$$

One disadvantage of the cylindrical cavity method is that only a single frequency point can be measured for one cavity, while the rectangular cavity has several TE_{10N} modes for measurements.

The main advantage of using perturbation techniques is that the requirement for the specimen size is very small; therefore the sample is easily prepared. The measurement error for ϵ_r is less than 2%. The measurement error for loss tangent is higher than that of the dielectric resonance techniques [25]. Loss tangent less than 1×10^{-3} is not recommended to be measured by this technique. Theoretically, the frequency limitation of the above two perturbation methods depends on the resonant frequencies of the cavities. For low frequencies, a long, uniform and small cross section sample is difficult to prepare. The limitation on the measurement of the real part of permittivity is that $\epsilon_r < 100$.

2.3.3. Re-entrant cavity. A different configuration of the perturbation technique is shown in figure 11 with $a \leq b$ [55–64]. The sample is located at the end of a cylindrical cavity. The two parallel surfaces of the sample are usually electroded to ensure good contact between the sample and the cavity. The method is called the re-entrant cavity technique. Like the lumped impedance technique, the electric field in the sample is assumed to be uniform. For high ϵ_r or high frequency conditions, this assumption will no longer be valid. The calculations of dielectric properties are also based on circuit theory. The resonance occurs when the impedance of the sample is the same as the impedance of the cavity with opposite sign

$$jZ_0 \tan \beta L = -\frac{1}{j\omega C_g}, \quad (22)$$

where Z_0 is the characteristic impedance of the cavity, β is the phase constant, L is the cavity length and C_g is the capacitance

Table 1. Summary of microwave dielectric property measurement techniques.

Methods	Frequency range (GHz)	Permittivity range	Loss resolution	Sample geometry	Swept frequency capability
Resonance techniques					
Dielectric resonance techniques					
Hakki–Coleman resonance	1–30 ^a	Broad range	$>1 \times 10^{-4}$	Cylinders no electrode	No
Cylindrical cavity resonance	1–20 ^a	Broad range	$>1 \times 10^{-5}$	Cylinders no electrode	No
Reflection resonance	1–20 ^a	Broad range	$>5 \times 10^{-5}$	Cylinders no electrode	No
Split-post resonance	>1	Broad range	$>2 \times 10^{-5}$	Laminas no electrode	No
Cavity resonance techniques					
TE cavity perturbation	>4	<100	$>1 \times 10^{-3}$	Thin rod, bar or slice	Yes/no
TM cavity perturbation	>4	<100	$>1 \times 10^{-3}$	Thin rod or bar	No
Re-entrant cavity	0.3–3	Low	$>1 \times 10^{-3}$	Electroded disk	No
Transmission/reflection techniques					
S_{11} and S_{21} reflection and transmission	Broad range	Broad range	$>10^{-2}$ – 10^{-3}	Cross section of holder	Yes
Longitudinal transmission	Broad range	Low	$>10^{-2}$ – 10^{-3}	Rectangular thin slice	Yes
Lumped impedance	<3	Low	$>10^{-2}$ – 10^{-3}	Electroded disk	Yes

^a Depends on ϵ_r .

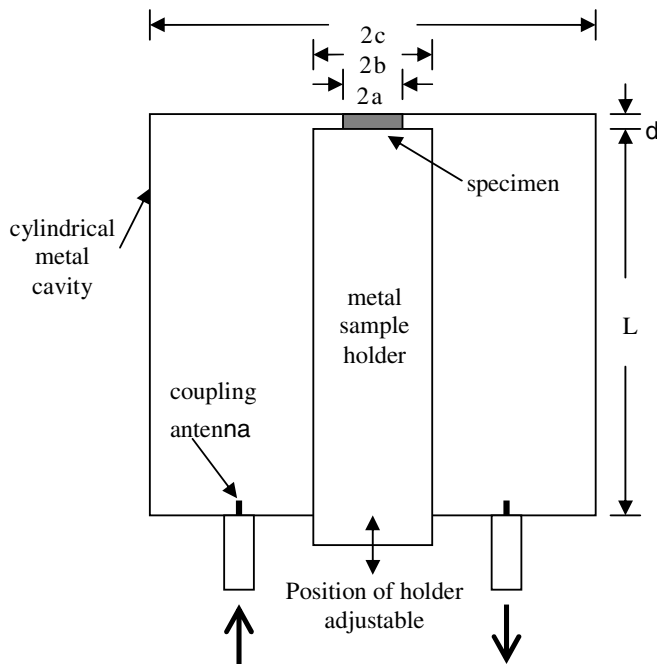


Figure 11. Re-entrant cavity perturbation technique.

of the gap region as a parallel plate capacitor:

$$Z_0 = \frac{\ln(c/b)}{2\pi} \sqrt{\frac{\mu_0}{\epsilon_0}}. \quad (23)$$

In the gap region where the sample is placed, the capacitance values without and with the sample are given by [55]

$$C_{go} = \frac{\epsilon_0 \pi a^2 + 4\epsilon_0 b \ln(c-b)}{d_0} \quad (24)$$

$$C_{gs} = \frac{\pi \epsilon_0 [a^2(\epsilon_r - 1) + b^2] + 4\epsilon_0 b \ln(c-b)}{d}, \quad (25)$$

respectively. d_0 is the gap width without the sample. The values of C_{go} and C_{gs} can be determined experimentally

from the resonant frequencies by equation (22). The real part of permittivity ϵ_r can then be calculated directly from equation (25).

If the center conductor (sample holder) of the cavity without the sample is adjusted (adjust d value) to the same frequency as that of the cavity with the sample, C_{go} is equal to C_{gs} . By equating the equations (24) and (25), we have the other equation to calculate the ϵ_r value.

The loss tangent is calculated using

$$\tan \delta = \frac{1}{Q} = \frac{1}{Q_s} - \frac{1}{Q_c}, \quad (26)$$

where Q_s and Q_c are the quality factors of the cavity with and without the samples at the same frequency, respectively. The frequency range of re-entrant cavities is typically from 300 MHz to 3 GHz depending on the size of the cavity designed.

2.4. Summary of microwave measurement techniques

A general review of some microwave measurement techniques has been given. Table 1 gives the summary of the different techniques discussed in this review. Different techniques were designed for the measurements of materials with different ϵ_r , loss tangents and sample geometries. Limitations for various techniques should be considered to choose the most suitable techniques for different purposes.

3. Experiments

To compare the accuracy and adequacy of various measurement techniques, the complex permittivities of three samples, polyethylene (Alfa Co.), alumina (Bolt Co.) and $\text{Ba}(\text{Mg}_{1/3}\text{Ta}_{2/3})\text{O}_3$ (Siemens Co.), were measured by five widely used transmission/reflection and resonance techniques discussed in this review. The measured results of the three materials are also compared with the data reported by other workers.

Table 2. Dielectric properties measured by various measurement techniques. The standard deviations of the measurements are also listed.

Materials	Techniques	Frequency (GHz)	ϵ_r	$\tan \delta$	Reference values			Refs.
					Frequency (GHz)	ϵ_r	$\tan \delta$	
Polyethylene	S_{11} and S_{21}	8.2–12.4	2.25 ± 0.09	**	26.5–40	2.34	–	[68]
	Cavity perturbation	8.2–12.4	2.29 ± 0.07	**	–	–	–	–
	Hakki–Coleman	10.1	2.32 ± 0.05	$(2.4 \pm 0.5) \times 10^{-4}$	–	–	–	–
	Cylindrical cavity	–	–	–	11.3	2.36 ± 0.06	$\sim(1.5 \pm 0.3) \times 10^{-4}$	[69]
	Others	–	–	–	10	2.25	4.0×10^{-4}	[70]
Alumina	S_{11} and S_{21}	8.2–12.4	–	–	0.05–18	~ 10	–	[12]
	Cavity perturbation	8.2–12.4	9.9 ± 0.4	**	–	–	–	–
	Hakki–Coleman	13.2	10.1 ± 0.3	$(1.0 \pm 0.4) \times 10^{-4}$	–	–	–	–
	Cylindrical cavity	8.4	9.8 ± 0.3	$(6 \pm 1) \times 10^{-5}$	12–18	–	3.0×10^{-4}	[71]
	Others	–	–	–	10	10.15	8.4×10^{-6}	[72]
		–	–	–	10	9.97	3.91×10^{-5}	[12]
–		–	–	10	9.5–10	3.0×10^{-4}	[70]	
Ba(Mg _{1/3} Ta _{2/3})O ₃	Cavity perturbation	8.2–12.4	25.0 ± 0.8	**	–	–	–	–
	Hakki–Coleman	17.7	24.4 ± 0.6	$(2.7 \pm 0.5) \times 10^{-4}$	7	25	9.80×10^{-5}	[73]
	Cylindrical cavity	–	–	–	10.5	25	–	[74]
		–	–	–	9	25.5	$(1.8–2.1) \times 10^{-4}$	[75]
		–	–	–	10	24.4	–	[76]
		–	–	–	10	–	1.0×10^{-4}	[76]
	Reflection	10.1	23.9 ± 0.6	$(1.5 \pm 0.3) \times 10^{-4}$	10.5	–	5.95×10^{-5}	[74]

** Below measurement resolution.

For the transmission/reflection methods, the S_{11} and S_{21} transmission and reflection technique was chosen because it has the least limitations on the measurements of ϵ_r and $\tan \delta$. Other transmission/reflection techniques were not chosen because the longitudinal transmission is only for low ϵ_r measurement and the lumped impedance technique is only applied to low frequency measurement. To compare the characteristics of transmission/reflection methods with resonant methods, four resonance techniques were adopted. The perturbation techniques are the most suitable for the measurements of small samples. The measurement results of the real part of permittivity by the perturbation technique and transmission techniques were compared. By comparing TM cavity and TE cavity techniques, the TE cavity technique was chosen because it can measure more frequency points than the TM cavity technique. Since the dielectric resonance techniques can measure loss tangent more accurately than other techniques, cylindrical cavity resonance and waveguide reflection resonance techniques were chosen for the purpose of loss tangent measurements. The measurement results of dielectric resonance techniques on the real part of permittivity and loss tangent by using the S_{21} signal (cylindrical cavity resonance) and the S_{11} signal (waveguide reflection resonance) can then be compared. However, for low ϵ_r samples, the sample dimensions are too large to fit inside the cavities for these two methods and the Hakki–Coleman technique was adopted instead [65].

The sample holder for the S_{11} and S_{21} technique was made by the standard X-band waveguide with a small section of thickness larger than or equal to the thickness of the specimen for measurements on a frequency band of 8.2 to 12.4 GHz. The sample was cut with the same dimensions as the waveguide inside the cross section (0.9 in \times 0.4 in); then the sample was slid into the sample holder. For the TE cavity perturbation method, one copper cavity was also fabricated by the standard X-band waveguide with length 13.5 cm for measurements on band frequencies 8.2 to 12.4 GHz. A cylindrical copper cavity with inside diameter 3 cm and height 1.7 cm and a rectangular copper waveguide section with cross section 4.75 cm \times 2.21 cm were used for the cylindrical cavity and waveguide reflection resonance techniques, respectively. For the Hakki–Coleman method, two brass plates with diameter 10 cm and conductivity 1.41×10^7 S m⁻¹ [28, 29] were adopted.

The measurement results are listed in table 2. As discussed before, the choice of the most appropriate measurement technique would depend on the characteristics of the measured sample. Some of the samples were not measured by the S_{11} and S_{21} technique because the available sample dimensions are too small to occupy the cross section of the X-band sample holder. As mentioned previously, some of the low ϵ_r samples were not measured by the cylindrical cavity resonance and the waveguide reflection techniques.

For the measurements in this review, good consistency was found in the measurements of the real part of permittivity among various techniques. Reasonable agreement was also obtained between the results in this review and the published data on the ϵ_r measurements. This confirms the measurement

accuracy on the real part of permittivity by the S_{11} and S_{21} technique, perturbation technique and resonance techniques.

For the measurement of loss tangents, the comparison of the results of this review with the published data is more difficult because the loss tangent strongly depends on the fabrication conditions. However, measurement results on loss tangent are essentially in the same range as the reported data. On the other hand, in the present work, acceptable agreement in the measurements of the loss tangent was reached between the cylindrical cavity resonance and the waveguide reflection techniques. The higher loss tangent values by the Hakki–Coleman technique than the cylindrical cavity and waveguide methods are reasonable because of the higher resonance frequencies. Usually, the loss tangent of ceramics will increase with increasing frequency at microwave frequencies [25, 66]. In summary, the measurement accuracy of these methods in measuring loss tangent values was verified. For the transmission/reflection technique, because of the limitation on loss tangent measurement, loss measurement was not conducted by this method.

The uncertainties (standard deviations) included in the table are from the measurement errors of frequency, half-power bandwidth, metal conductivity and dimensions as well as the repeatability uncertainty. The errors of the real part of permittivity are mainly from the uncertainties of sample dimension measurement and repeatability. The errors of the Hakki–Coleman resonance method are from the measurement error of the surface resistance and half-power bandwidth. As mentioned, the conductor losses of the cylindrical cavity and the waveguide reflection methods are much lower than those of the Hakki–Coleman technique. The accuracy for loss measurement of these two techniques is higher. This phenomenon can be verified by the loss tangent measurements of alumina and Ba(Mg_{1/3}Ta_{2/3})O₃. The uncertainty of half-power bandwidth measurement also contributes a measurement error to the cylindrical cavity and reflection techniques. The higher error for the reflection method than the cylindrical cavity is due to, in addition to the bandwidth error, the uncertainty of power level measurement in figure 7 [25, 67].

4. Conclusions

A general review and comparison between the resonance techniques and the transmission/reflection techniques of microwave dielectric property measurements was given. For the transmission/reflection techniques, the main advantage is the capability of swept frequency; however, their capability for loss measurement is limited. For the resonance techniques, four dielectric resonance techniques and three cavity perturbation techniques have been discussed and compared. The dielectric resonance methods are the better choice for loss tangent measurement. The cavity perturbation technique is good for measurement of the real part of permittivity and the required specimen is very small but is not adequate for extremely low loss tangent measurement. The Hakki–Coleman resonance technique can measure both the real part of permittivity and loss tangent. The cylindrical

cavity resonance, split post-resonance and the waveguide reflection techniques have the best accuracy on loss tangent measurement. The choice of the measurement technique will depend on the available sample dimension, dielectric properties and the accuracy requirement.

Five measurement techniques are chosen from two types of measurement methods. Experiments are conducted on these techniques and the results show that good measurement agreement can be reached among the transmission techniques and the resonance techniques.

Acknowledgment

This work was partially supported by the National Science Council of the Republic of China, Taiwan under Contract No. NSC 94-2213-E-150-037.

References

- [1] Krupka J 2006 Frequency domain complex permittivity measurements at microwave frequencies *Meas. Sci. Technol.* **17** R55–70
- [2] Baker-Jarvis J, Janezic M D, Riddle B F, Johnk R T, Kabos P, Holloway C L, Geyer R G and Grosvenor C A Measuring the permittivity and permeability of lossy materials: solids, liquids, metals, building materials, and negative-index materials *NIST Technical Note* 1536
- [3] Clarke R N 2004 *A Guide to the Characterisation of Dielectric Materials at RF and Microwave Frequencies* (Teddington: NPL)
- [4] Chen L F, Ong C K, Neo C P, Varadan V V and Varadan V 2004 *Microwave Electronics: Measurement and Materials Characterization* (New York: Wiley)
- [5] Egorov V N 2007 Resonance methods for microwave studies of dielectrics (review) *Instrum. Exp. Tech.* **50** 143–75
- [6] Baker-Jarvis J 1990 Transmission/reflection and short-circuit line permittivity measurements *NIST Technical Note* 1341
- [7] Baker-Jarvis J, Vanzura E J and Kissick W A 1990 Improved technique for determining complex permittivity with the transmission/reflection method *IEEE Trans. Microw. Theory Tech.* **38** 1096–103
- [8] Van den Broeck T, Dhondt G, Barel A and Martens L 1996 Parametric modelling of complex permittivity and permeability *IEEE MTT-S Dig.* **3** 1419–21
- [9] Ligthart L P 1983 A fast computational technique for accurate permittivity determination using transmission line methods *IEEE Trans. Microw. Theory Tech.* **31** 249–54
- [10] Nicolson A M and Ross G F 1970 Measurement of the intrinsic properties of materials by time-domain techniques *IEEE Trans. Instrum. Meas.* **19** 377–82
- [11] Weir W B 1974 Automatic measurement of complex dielectric constant and permeability at microwave frequencies *Proc. IEEE* **62** 33–6
- [12] Vanzura E J, Baker-Jarvis J R, Grosvenor J H and Janezic M D 1994 Intercomparison of permittivity measurements using the transmission/reflection method in 7-mm coaxial transmission lines *IEEE Trans. Microw. Theory Tech.* **42** 2063–70
- [13] Dube D C, Lanagan M T and Jang S J 1987 Dielectric measurements of package materials in an inhomogeneously filled rectangular waveguide *J. Am. Ceram. Soc.* **70** C278–80
- [14] Catala-Civera J M, Canos A J, Penaranda-Foix F L and De Los Reyes Davo E 2003 Accurate determination of the complex permittivity of materials with transmission reflection measurements in partially filled rectangular waveguides *IEEE Trans. Microw. Theory Tech.* **51** 16–24
- [15] Lanagan M T, Kim J H, Jang S J and Newnham R E 1988 Microwave dielectric properties of antiferroelectric lead zirconate *J. Am. Ceram. Soc.* **71** 311–6
- [16] Lanagan M T, Kim J H, Dube D C, Jang S J and Newnham R E 1988 A microwave dielectric measurement technique for high permittivity materials *Ferroelectrics* **82** 91–7
- [17] Sabisky E S and Gerritsen H J 1962 Measurement of the dielectric constant of rutile (TiO₂) at microwave frequencies between 4.2 and 300 K *J. Appl. Phys.* **33** 1450–3
- [18] Afsar M N, Wang Y and Andreucci A N 2002 Accurate measurement of complex permittivity of liquids using the in-waveguide technique *CPEM Digest (Conf. on Precision Electromagnetic Measurements)* pp 6–7
- [19] Hayashi Y, Mishima G, Hirayama K and Hayashi Y 2003 Simultaneous measurement of permittivity and permeability of lossy sheet using flanged rectangular waveguide *Electron. Commun. Japan, Part II: Electronics* **86** 32–41
- [20] Afsar M N, Suwanvisan N and Wang Y 2006 Permittivity measurement of low and high loss liquids in the frequency range of 8 to 40 GHz using waveguide transmission line technique *Microw. Opt. Tech. Lett.* **48** 275–81
- [21] Stuchly S S, Pzepecka M A and Iskander M F 1974 Permittivity measurements at microwave frequencies using lumped elements *IEEE Trans. Instrum. Meas.* **23** 56–62
- [22] Pzepecka M A and Stuchly S S 1975 A lumped capacitance method for the measurement of the permittivity and conductivity in the frequency and time domain—a further analysis *IEEE Trans. Instrum. Meas.* **24** 27–32
- [23] Iskander M F and Stuchly S S 1978 Fringing field effect in the lumped-capacitance method for permittivity measurement *IEEE Trans. Instrum. Meas.* **27** 107–9
- [24] Anderson L, Stuchly S S and Gajda G B 1986 Parallel-plate coaxial sensor for dielectric measurements—further analysis *IEEE Trans. Instrum. Meas.* **35** 89–91
- [25] Sheen J 2005 Study of microwave dielectric properties measurements by various resonance techniques *Measurement* **37** 123–30
- [26] Sucher M 1963 *Handbook of Microwave Measurements* vol 2 ed M Sucher and J Fox (New York: Brooklyn Polytechnic Press) chapter 8
- [27] Kwok R S and Liang J F 1999 Characterization of high-Q resonators for microwave-filter applications *IEEE Trans. Microw. Theory Tech.* **47** 111–4
- [28] Kobayashi Y and Katoh M 1985 Microwave measurement of dielectric properties of low-loss materials by the dielectric rod method *IEEE Trans. Microw. Theory Tech.* **33** 586–92
- [29] Xu D and Li Z 1985 A novel method for characterizing the surface resistance of two conducting plates shorted at both ends of a dielectric resonators *15th European Microwave Conf. Proc.* pp 912–6
- [30] Hakki B W and Coleman P D 1960 A dielectric resonator method of measuring inductive capacities in the millimeter range *IRE Trans. Microw. Theory Tech.* **8** 402–10
- [31] Courtney W E 1970 Analysis and evaluation of a method of measuring the complex permittivity and permeability of microwave insulators *IEEE Trans. Microw. Theory Tech.* **18** 476–85
- [32] Tamura H, Hatsumoto H and Wakino K 1989 Low temperature properties of microwave dielectrics *Japan. J. Appl. Phys.* **28** (Suppl. 28-2) 21–3
- [33] Konaka T, Sato M, Asano H and Kubo S 1991 Relative permittivity and dielectric loss tangent of substrate materials for high-T_c film *J. Supercond.* **4** 283–8
- [34] Lui M L and Wu K L 2004 An efficient volume integral equation approach for characterization of lossy dielectric materials *IEEE Trans. Microw. Theory Tech.* **MTT-52** 2464–73

- [35] Prokopenko Yu V and Filipov Yu F 2002 Anisotropic disk dielectric resonator with conducting end faces *Tech. Phys.* **47** 731–6
- [36] Barannik A A, Prokopenko Yu V, Filipov Yu F, Cherpak N T and Korotash I V 2003 Q factor of a millimeter-wave sapphire disk resonator with conductive end plates *Tech. Phys.* **48** 621–5
- [37] Akay M F, Prokopenko Yu and Kharkovsky S 2004 Resonance characteristics of whispering gallery modes in parallel-plates-type cylindrical dielectric resonators *Microw. Opt. Tech. Lett.* **40** 96–101
- [38] Cherpak N T, Barannik A A, Prokopenko Yu V, Filipov Yu F and Vitusevich S 2003 Accurate microwave technique of surface resistance measurement of large-area HTS films using sapphire quasi-optical resonator *IEEE Trans. Appl. Supercond.* **13** 3570–3
- [39] Guillon P and Garault Y 1977 Accurate resonant frequencies of dielectric resonators *IEEE Trans. Microw. Theory Tech.* **MTT-25** 916–22
- [40] Krupka J, Gregory A P, Rochard O C, Clarke R N, Riddle B and Baker-Jarvis J 2001 Uncertainty of complex permittivity measurements by split-post dielectric resonator technique *J. Eur. Ceram. Soc.* **21** 2673–6
- [41] Krupka J 1988 Properties of shielded cylindrical quasi-TE_{0nm}-mode dielectric resonators *IEEE Trans. Microw. Theory Tech.* **MTT-36** 774–9
- [42] Krupka J, Derzakowski K, Riddle B and Baker-Jarvis J 1998 A dielectric resonator for measurements of complex permittivity of low loss dielectric materials as a function of temperature *Meas. Sci. Technol.* **9** 1751–6
- [43] Krupka J, Huang W-T and Tung M-J 2005 Complex permittivity measurements of low loss microwave ceramics employing higher order quasi TE_{0np} modes excited in a cylindrical dielectric sample *Meas. Sci. Technol.* **16** 1014–20
- [44] Sheen J 2007 Microwave measurements of dielectric properties using a closed cylindrical cavity resonator *IEEE Trans. Dielectr. Electr. Insul.* **14** 1139–44
- [45] Plourde J K, Linn D F, O'Bryan H M Jr and Thomson J Jr 1975 Ba₂Ti₉O₂₀ as a microwave dielectric resonator *J. Am. Ceram. Soc.* **58** 418–20
- [46] Onoda M, Kuwata J, Kaneta K, Toyama K and Nomura S 1982 Ba(Zn_{1/3}Nb_{2/3})O₃-Sr(Zn_{1/3}Nb_{2/3})O₃ solid solution ceramics with temperature-stable high dielectric constant and low microwave loss *Japan. J. Appl. Phys.* **21** 1707–10
- [47] Sheen J 2007 Microwave dielectric properties measurements using the waveguide reflection dielectric resonator *Proc IEEE Instrumentation and Measurement Technology Conf., IMTC (Warsaw, Poland, 1–3 May)* pp 1–4
- [48] Split post dielectric resonators for dielectric measurements of substrates *Agilent Application Note* 5989-5384EN
- [49] Krupka J, Gabelich S A, Derzakowski K and Pierce B M 1999 Comparison of split post dielectric resonator and ferrite disc resonator techniques for microwave permittivity measurements of polycrystalline yttrium iron garnet *Meas. Sci. Technol.* **10** 1004–8
- [50] Mazierska J, Krupka J, Jacob M V and Ledenyov D 2004 Complex permittivity measurements at variable temperatures of low loss dielectric substrates employing split post and single post dielectric resonators *IEEE MTT-S Int. Microw. Symp. Digest* vol 3 pp 1825–8
- [51] Sheen J 2007 Amendment of cavity perturbation technique for loss tangent measurement at microwave frequencies *J. Appl. Phys.* **102** 014102
- [52] Dube D C, Lanagan L T, Kim J H and Jang S J 1988 Dielectric measurements on substrate materials at microwave frequencies using cavity perturbation technique *J. Appl. Phys.* **63** 2466–8
- [53] Nakamura E and Furuichi J 1960 Measurement of microwave dielectric constants of ferroelectrics *J. Phys. Soc. Japan.* **15** 1955–60
- [54] Yamamoto J K, Lanagan M T, Bhalla A S, Newnham R E and Cross L E 1989 Dielectric properties of microporous glass in the microwave region *J. Am. Ceram. Soc.* **72** 916–21
- [55] Xi W, Tinga W R, Voss W A G and Tian B Q 1992 New results for coaxial re-entrant cavity with partially dielectric filled gap *IEEE Trans. Microw. Theory Tech.* **40** 747–53
- [56] Baker-Jarvis J and Riddle B 1996 Dielectric measurements using a reentrant cavity: mode-matching analysis *NIST Technical Note* 1384
- [57] Goodwin A R H, Mehl J B and Moldover M R 1996 Reentrant radio-frequency resonator for automated phase-equilibria and dielectric measurements in fluids *Rev. Sci. Instrum.* **67** 4292–303
- [58] Kelly M B and Sangster A J 1997 Design of cylindrical re-entrant cavity resonators *IEE Colloq. Effect. Microw. CAD* **3/1–3/4**
- [59] Vints M and Hellemans L 1988 The measurement of non-linear dielectric effects with re-entrant cavities *5th Int. Conf. on Dielectric Materials, Measurements and Applications (27–30 June)* pp 340–3
- [60] Kanai T, Tsukamoto T, Miyakawa M and Kashiwa T 2000 Resonant frequency analysis of reentrant resonant cavity applicator by using FEM and FD-TD method *IEEE Trans. Magn.* **36** 1750–3
- [61] Barroso J J, Castro P J, Leite Neto J P and Aguiar O D 2005 Reentrant cylindrical cavities *SBMO/IEEE MTT-S Int. Conf. on Microwave and Optoelectronics (25–28 July)* pp 129–32
- [62] Kaczkowski A and Milewski A 1980 High-accuracy wide-range measurement method for determination of complex permittivity in reentrant cavity: part A—theoretical analysis of the method *IEEE Trans. Microw. Theory Tech.* **28** 225–8
- [63] Kaczkowski A and Milewski A 1980 High-accuracy wide-range measurement method for determination of complex permittivity in reentrant cavity: part B—experimental analysis of measurement error *IEEE Trans. Microwave Theory Tech.* **28** 228–31
- [64] Sen S, Saha P K and Nag B R 1979 New cavity perturbation technique for microwave measurement of dielectric constant *Rev. Sci. Instrum.* **50** 1594–7
- [65] Sheen J 2006 Losses of the parallel plate dielectric resonator *Proc. IEEE Instrumentation and Measurement Technology Conf., IMTC (Sorrento, Italy, 24–27 April 2006)* pp 2184–7
- [66] Wakino K, Murata M and Tamura H 1986 Far infrared reflection spectra of Ba(Zn,Ta)O₃-BaZrO₃ dielectric resonator material *J. Am. Ceram. Soc.* **69** 34–7
- [67] Ridler N, Lee B, Martens J and Wang K 2007 Measurement, uncertainty, traceability, and the GUM *IEEE Microw. Mag.* **8** 44–53
- [68] Seeger K 1991 Microwave measurement of the dielectric constant of high-density polyethylene *IEEE Trans. Microw. Theory Tech.* **39** 352–4
- [69] Riddle B, Baker-Jarvis J and Krupka J 2003 Complex permittivity measurements of common plastics over variable temperatures *IEEE Trans. Microw. Theory Tech.* **51** 727–33
- [70] Pozar D M 1998 *Microwave Engineering* 2nd edn (New York: Addison-Wesley) p 705
- [71] Molla J, Ibarra A, Margineda J, Zamorro J M and Hernandez A 1993 Dielectric property measurement system at cryogenic temperatures and microwave frequencies *IEEE Trans. Instrum. Meas.* **42** 817–21
- [72] Breeze J D, Aupi X and Alford N McN 2002 Ultralow loss polycrystalline alumina *Appl. Phys. Lett.* **81** 5021–3

- [73] Tamura H, Konoike T, Sakabe Y and Wakino K 1984 Improved high-Q dielectric resonator with complex perovskite structure *Commun. Am. Ceram. Soc.* **67** C59–61
- [74] Nomura S, Toyama K and Kaneta K 1982 Ba(Mg_{1/3}Ta_{2/3})O₃ ceramics with temperature-stable high dielectric constant and low microwave loss *Japan. J. Appl. Phys.* **21** 624–6
- [75] Wu Y J and Chen X M 2003 Microwave dielectric characteristics of Ba(Mg_{1/3}Ta_{2/3})O₃ ceramics sintered at low-temperatures *Mater. Eng. B* **100** 244–7
- [76] Sebastian M T and Surendran K P 2006 Tailoring the microwave dielectric properties of Ba(Mg_{1/3}Ta_{2/3})O₃ ceramics *J. Eur. Ceram. Soc.* **26** 1791–9